

# Production of Radioactive Nuclides in Inverse Reaction Kinematics

E. Traykov<sup>a</sup>, A. Rogachevskiy<sup>a</sup>, U. Dammalapati<sup>a</sup>,  
P. Dendooven<sup>a</sup>, O.C. Dermois<sup>a</sup>, K. Jungmann<sup>a</sup>,  
C.J.G. Onderwater<sup>a</sup>, M. Sohani<sup>a</sup>, L. Willmann<sup>a</sup>,  
H.W. Wilschut<sup>a,1</sup>, A.R. Young<sup>b</sup>

<sup>a</sup>*Kernfysisch Versneller Instituut, Rijksuniversiteit Groningen,  
Zernikelaan 25, 9747 AA Groningen, The Netherlands*

<sup>b</sup>*Department of Physics, NC State University, Box 8202 Raleigh, NC 27695 USA*

---

## Abstract

Efficient production of short-lived radioactive isotopes in inverse reaction kinematics is an important technique for various applications. It is particularly interesting when the isotope of interest is only a few nucleons away from a stable isotope. In this article production via charge exchange and stripping reactions in combination with a magnetic separator is explored. The relation between the separator transmission efficiency, the production yield, and the choice of beam energy is discussed. The results of some exploratory experiments will be presented.

*PACS: 07.55.-w; 07.55.+h; 29.30.-h; 41.85.-p; 41.75.-i; 25.70.-z;*

*Keywords: Magnetic separator, Inverse reaction kinematics, Secondary radioactive isotopes*

---

## 1 Introduction

Beams of radioactive nuclides can be produced in several ways. Various strategies have been explored extensively, in particular as starting points for the next generation of large scale radioactive beam facilities such as FAIR [1], RIA [2] and SPIRAL II [3]. A special case is the production of nuclides that can be reached in simple “rearrangement reactions”, such as charge exchange

---

<sup>1</sup> Corresponding author,  
Fax: +31-50-3633600,  
E-mail: wilschut@kvi.nl

reactions, e.g. (p,n) reactions, and stripping reactions, e.g. (d,p) and (d,n) reactions. By inverting the kinematics of the reactions, i.e. using a light particle target ( $H_2$ ,  $D_2$ ,  $^3,^4He$ ) and a heavy-ion beam, secondary beams can be obtained with considerable intensity and favorable emittance. Such beams have been successfully exploited, for example at Argonne National Laboratories [4] for astrophysical studies. At the Cyclotron Institute of Texas A&M the inverse reaction technique is used at the MARS spectrometer [5] for  $\beta$ -decay studies. For the TRI $\mu$ P facility at KVI Groningen, Netherlands, these secondary beams will be used to study fundamental symmetries and interactions via  $\beta$ -decay of light nuclei [6].

Recently, one key part of the facility, the TRI $\mu$ P separator, has become operational [7]. The TRI $\mu$ P separator consists of two dipole sections. The first one separates the primary and secondary beam, with the secondary beam dispersed in the intermediate focal plane. The second section brings the secondary beam back to an achromatic focus at the exit of the separator. One can add an absorber in the intermediate plane, which allows one to remove unwanted products that are produced with the same rigidity as the desired secondary beam. In this sense the TRI $\mu$ P separator is like the magnetic separators used for fragmentation reactions [10,11]. In combination with reactions in inverse kinematics clean and intense beams can be obtained with such separators. Intensity limitations arise from the separator acceptance both in momentum and angle.

In this article we explore in which way we can minimize the impact of the separator acceptance. In particular, whether to choose low or high energy beams. The various concepts to exploit inverted reaction kinematics were tested experimentally. The methods were applied already in the implantation of radioactive nuclides in Si detectors, to study  $\beta$ -decay for fundamental and astrophysical research [8,9].

## 2 Kinematics

First we consider the momentum and angular acceptance. For the purpose of our discussion it is sufficient to use non-relativistic kinematics. The maximal variation in momentum,  $\Delta p/p$  of the projectile-like particle produced in a binary reaction is (see figure 1)

$$\frac{\Delta p}{p} = \frac{2P_R}{P_{CMS}}, \quad (1)$$

where  $P_{CMS}$  is the momentum associated with the center-of-mass motion and  $P_R$  is the recoil momentum in the center of mass. The projectile-like particles

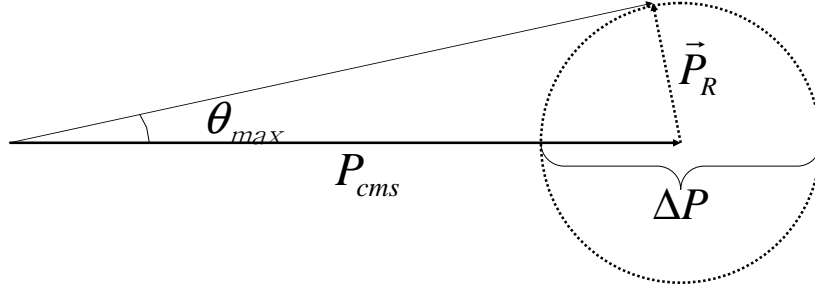


Fig. 1. Schematic diagram of the emittance of reaction products in inverse kinematics.

are emitted within a cone of

$$\Delta\theta = 2\theta_{max} = 2 \arcsin \frac{P_R}{P_{CMS}} \approx \frac{2P_R}{P_{CMS}}. \quad (2)$$

Thus  $\Delta\theta \approx \Delta p/p$ . In terms of masses of the projectile ( $A_P$ ), target ( $A_T$ ), projectile-like particle ( $A_{PLF}$ ), and target-like particle ( $A_{TLF}$ )

$$\frac{\Delta p}{p} = 2\sqrt{\frac{A_{TLF}A_T}{A_{PLF}A_P}\left(1 + \frac{Q}{E_{cm}}\right)}, \quad (3)$$

where  $Q$  is the energy excess (Q-value) of the reaction and  $E_{cm}$  is the center-of-mass energy. Thus in reactions where  $|Q| \ll E_{cm}$ , such as in direct reactions, the momentum distribution depends only on the masses. For example, in a (p,n) reaction  $\Delta p/p \approx 2/A_P$ . Another important result of equation (3) is that reactions with a large negative Q-value will have small emittance. Moreover, when  $-Q$  is much larger than the Coulomb barrier in the entrance channel, the reaction cross section nearly always peaks at threshold, mostly because the reaction typically proceeds via a resonant state in the compound nucleus.

Next we consider the angular distribution. We can write

$$\frac{d\sigma}{dp} = \frac{d\sigma}{d\Omega} 2\pi \sin \theta' \cdot \frac{p}{P_{CMS}P_R \sin \theta'}, \quad (4)$$

where  $\theta'$  is the center-of-mass angle and  $p$  the laboratory momentum of the projectile-like particle. When the center-of-mass angular distribution  $d\sigma/d\Omega$  is isotropic the resulting momentum distribution is box shaped, i.e.

$$\frac{d\sigma}{dp} \propto \frac{p}{P_{CMS}P_R} \text{ for } P_{CMS} - P_R \leq p \leq P_{CMS} + P_R. \quad (5)$$

When the angular distribution approaches a  $1/\sin \theta'$  dependence, singularities appear in the momentum distribution at the limits  $p = P_{CMS} \pm P_R$ .

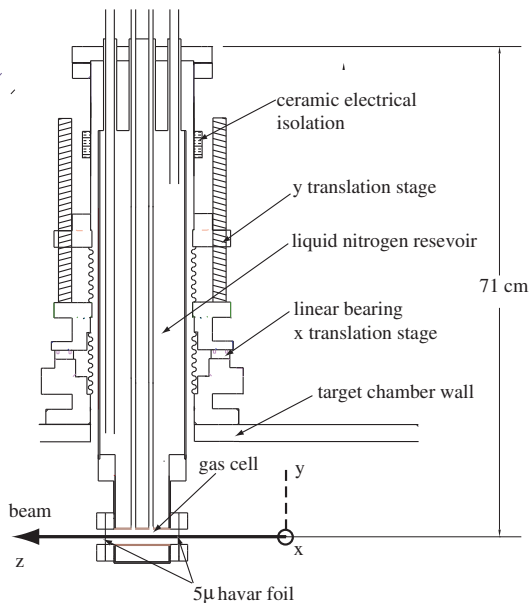


Fig. 2. Schematic drawing of the gas target

### 3 Gas target

For the production technique using inverse reactions a gas target is essential. At high beam intensities a solid or liquid target of e.g. Hydrogen would dissipate so much heat locally that it would go into the gas phase. Also, a solid target with hydrogen, like polyethylene, would lose rapidly its hydrogen content.

The target for the TRI $\mu$ P facility is based on a design from Texas A&M [12] and has been built at North Carolina State University [13]. The target has been used so far with 1 bar of H<sub>2</sub> and with D<sub>2</sub>. It is kept at liquid Nitrogen temperature in a 10 cm long volume closed by windows of 5  $\mu$ m Havar of 1 cm diameter. The resulting target thickness is 3.2 mg/cm<sup>2</sup> for H<sub>2</sub>. The beam diameter at the target position is typically 2-3 mm. A schematic drawing of the target configuration is shown in figure 2. The target can be moved remotely to allow the use of other targets (e.g. a viewing target). The target is electrically isolated to allow target-current read-out. The liquid-nitrogen dewar is automatically filled. The target has been operated successfully in all experiments so far, without replacing the windows.

### 4 Reactions near threshold

We have measured  $d\sigma/dp$  for a number of reactions. Here we discuss results for the reaction  $p(^{20}\text{Ne}, ^{20}\text{Na})n$  at 22.3 MeV/nucleon ( $E_{cm} = 21.4$  MeV) with

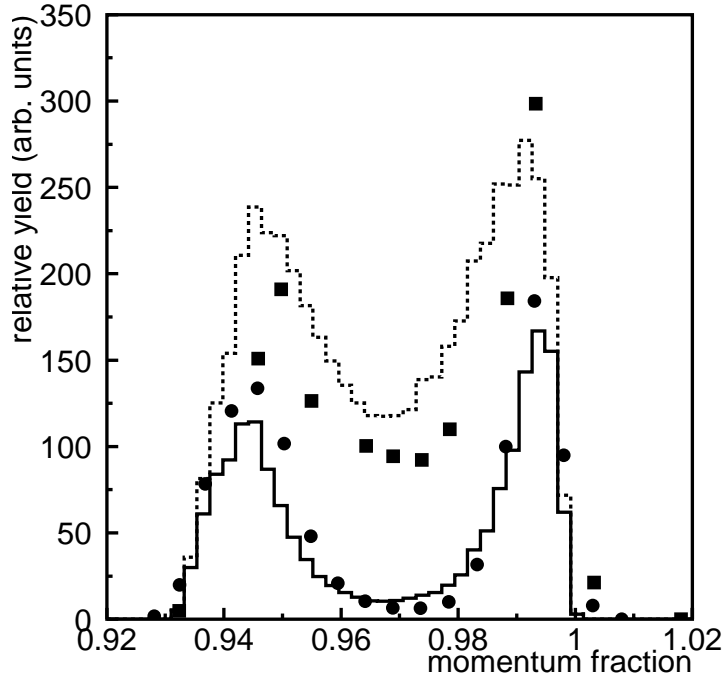


Fig. 3. Momentum dependence of the measured  $^{20}\text{Na}$  yield for two angular openings of the separator. The filled circles correspond to an angular opening of 32 mrad and the filled squares to the maximum angular opening of 60 mrad. The histograms show the result of Monte Carlo simulations assuming isotropic emission. The full and dashed histogram refer to the small and large opening respectively. The relative normalization of the two data sets is uncertain due to systematic errors of about 20%.

a Q-value of -14.7 MeV. The average center-of-mass energy correcting for various energy losses is 20.7 MeV. This implies for this reaction that on average  $\Delta\theta = 54$  mrad and  $\Delta p/p = 5.4\%$ , cf. equation (2). The emittance is thus close to the acceptance of the separator, which is 60 mrad and 4% in angle and momentum, respectively. Had the Q-value been zero the emittance would have been  $\approx 2/A_P$  or 100 mrad and 10%, respectively, i.e. 60% larger than for the actual Q-values. This illustrates the effect of the large negative Q-value.

To measure  $d\sigma/dp$  we scanned the rigidity of the separator, using a Si detector with a 2 cm diameter in the intermediate focal plane of the device. Two scans were performed: One with the full angular opening and one with the angular acceptance restricted to 32 mrad. In figure 3 we show the measured  $d\sigma/dp$  for these two acceptances. For comparison we also give the results of Monte Carlo simulations of an isotropic distribution that includes the effect of stopping and straggling in the target and the beam divergence. The calculations were normalized to the high momentum part of the scan with a small angular opening. Systematic errors are about 20%. The data and calculations show that the

momentum dependence of the yield distribution can be well understood. The differences with the data are in part due to the fact that the actual angular distribution is not isotropic [14] and part due to the finite size of the detector.

## 5 Direct reactions

In the following we consider the effect of the angular distribution on the kinematic focusing. Here we are concerned with the shape of the angular distribution and its dependence on beam energy. For (p,n) reactions this has been studied extensively and a parametrization of the shape of the distribution is available [16,17]. The cross sections decrease approximately as  $1/E_{cm}$  well above threshold, while the angular distribution becomes more focused at forward angles. We will argue below in section 6 that the target thickness can be increased until the phase space of the separator is fully used, which allows one to compensate the  $1/E$  dependence of the cross section.

The increasing acceptance with increasing energy does not stem from the higher energy itself (see section 2) but from the fact that the angular distribution is peaked more strongly around  $0^\circ$ . For (p,n) reactions this can be shown explicitly. Here the angular distribution depends on the momentum transfer,  $q^2 \approx k^2 \sin^2 \theta' / 2$ , with  $k$  the beam momentum per nucleon. The cross section is approximated by [16]

$$\frac{d\sigma}{dq} = \frac{2\pi}{k^2} \sigma_0 q \exp(-q^2 \langle r^2 \rangle / 3), \quad (6)$$

where  $\langle r^2 \rangle$  is the mean square radius of the projectile. The main point is that the cross section only depends on the momentum transfer and that this holds at least qualitatively over a large energy range. With this assumption the secondary beam emittance decreases as  $1 - \exp(-q_{max}^2 \langle r^2 \rangle / 3)$ , where  $q_{max}$  is determined by  $\theta_{max}$ . For other direct reactions a qualitatively similar emittance decrease with beam energy can be safely assumed. The measured differential distribution of the yield as function of the rigidity of the separator is

$$\frac{d\sigma}{dp} = \frac{P_{RP}}{P_{CMS} q} \frac{d\sigma}{dq} \propto \frac{P_{RP}}{P_{CMS}} \exp(-q^2 \langle r^2 \rangle / 3), \quad (7)$$

where the last proportionality is only valid for (p,n) reactions.

We have measured the momentum dependence for two typical reactions, the reaction  $p(^{21}\text{Ne}, ^{21}\text{Na})n$  at 43 MeV/nucleon and the reaction  $d(^{20}\text{Ne}, ^{21}\text{Na})n$  at 22.3 MeV/nucleon. The Q-value for these reactions are -4.3 and 0.2 MeV,

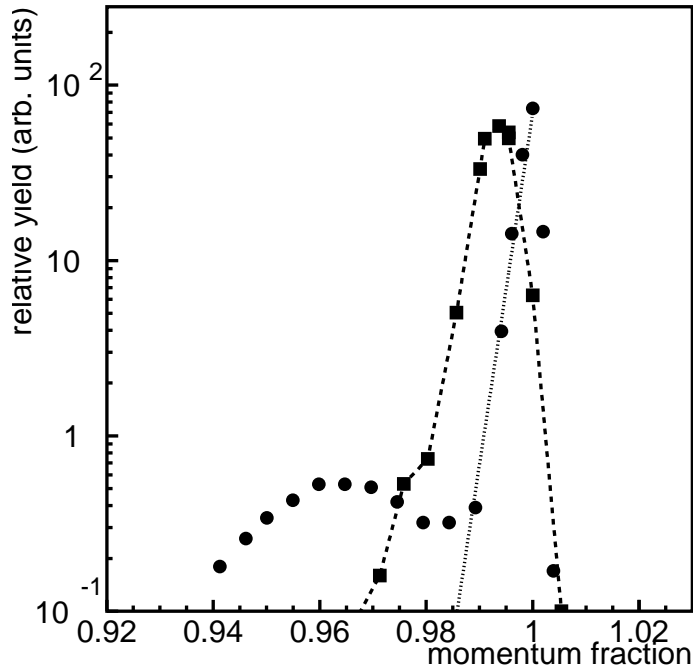


Fig. 4. Momentum dependence of the reactions  $p(^{21}\text{Ne}, ^{21}\text{Na})n$  at 43 MeV/nucleon and  $d(^{20}\text{Ne}, ^{21}\text{Na})n$  at 22.3 MeV/nucleon. The result for the first reaction is indicated by the filled circles. The dotted line through the sharp rising part of the distribution is a fit using equation (7). The filled squares give the distribution of the stripping reaction; the dashed line connecting these data points is to guide eye.

respectively, i.e. both reactions are well above threshold. The first reaction has high yields because  $^{21}\text{Ne}$  and  $^{21}\text{Na}$  are mirror nuclei. The production using the stripping reaction proceeds preferentially via states with strong single particle nature. Terakawa et al. [15] found the largest population in the first excited state of  $^{21}\text{Na}$  which corresponds to the  $d(5/2)$  state.

The measured momentum distributions are presented in fig. 4. They were obtained in the same setup as described above. The strong forward focus is very prominent in both reactions. The main yield is in a momentum range of only 1 to 2 %. For the (p,n) reaction the rising yield has been fitted with equation (7) using  $\langle r^2 \rangle$  as a free parameter. A reduced radius  $r_0 = 1.45$  fm was found, which is a satisfactory result in view of the approximations and the experimental method. The shape of the low yield tail for this reaction is due to the combined effect of the changing acceptance of the separator on one hand, and the characteristic oscillations in the angular distributions at large angle on the other. Also the stripping reaction shows a steep fall. In this case, however, the energy straggling defines most of the shape of the distribution. The window for the angular distribution extends only up to  $25^\circ$  in the center of mass. Nonetheless, it exhausts a large fraction of the total yield as can be

inferred from ref. [15], which reports on angular distribution measurements at the much lower energy of 12.5 MeV/nucleon.

## 6 Target thickness

The yield in inverse kinematics can be maximized by increasing the target thickness. However, at some point the added production will fall outside the acceptance of the separator. One of the important parameters is the stopping power. Because both beam and product are slowed down, only the difference in stopping power needs to be considered. One has exhausted the acceptance of the magnetic separator when the thickness  $d$  leads to a differential energy loss

$$\Delta E_{diff} = \left(1 - \left(\frac{Z_{product}}{Z_{beam}}\right)^2\right) d \left(\frac{dE}{dx}\right)_{beam} \quad (8)$$

that is larger than the energy acceptance of the separator. In equation (8) we have used the  $Z^2$  dependence of the stopping power  $dE/dx$ . Note that the entrance and exit windows play no role. However, the amount of angular and energy straggling, of course, does increase with the amount of material.

Integrating over the momentum dependence in equation (6) one obtains

$$\sigma \approx \frac{3\pi}{k^2} \frac{\sigma_0}{\langle r^2 \rangle} \approx 200 \text{ [MeV}\cdot\text{fm}^2] \frac{\sigma_0}{\mu^2 \langle r^2 \rangle \epsilon}, \quad (9)$$

where  $\mu$  is the reduced mass in a.m.u. and  $\epsilon$  is the beam energy per nucleon. The maximum yield is then

$$Y_{max} = I\sigma d = \frac{I(\sigma E)(\Delta E/E)}{\left(1 - \left(\frac{Z_{product}}{Z_{beam}}\right)^2\right) \left(\frac{dE}{dx}\right)_{beam}}, \quad (10)$$

where  $I$  is the beam current and  $\Delta E/E$  is the energy acceptance of the separator (8% for the TRI $\mu$ P separator). In the denominator of this equation the compensation of the energy dependence of the cross section is made explicit. Moreover, the stopping power in the nominator has also a  $1/E$  dependence, in this energy range. Thus if a production cross section is the result of a direct reaction the highest beam energy should be considered. For a (p,n) reaction only the constraints of the accelerator are a limiting factor. Typical production rates of the (p,n) and (d,p) reactions discussed were  $3.2 \times 10^3$  and  $1.3 \times 10^4$  /s/particle-nA, respectively.



Using equation (10) to extrapolate towards higher yields we find that increasing the target pressure 10-fold, eliminating current constraints on the separator acceptance, and considering the foreseen upgrade in beam current, a production rate of  $10^9$  radioactive particles/s can be reached with the TRI $\mu$ P separator in selected reactions.

## 7 Conclusions

We have considered two methods to produce efficiently a secondary beam of radioactive particles. The methods are based on using a light target and heavy-ion beam. The first method can be used in reactions that have a large negative Q-value. One can select beam energies near threshold, which results in small recoil energies, while the products remain fast enough to allow to transmit and separate them efficiently in a magnetic separator. The second method exploits the increasingly narrow angular distributions. Both methods can be roughly modelled so that these models can be used to optimize the settings of the separator, using e.g. the LISE code [18]. The methods described here can be used to produce beams with rather narrow energy distributions, which can be used as a starting point for radioactive beam experiments.

## 8 Acknowledgments

This work was supported by the *Rijksuniversiteit Groningen* and the *Stichting voor Fundamenteel Onderzoek der Materie* (FOM) under program 48 (TRI $\mu$ P). We thank the members of the AGOR cyclotron group and the KVI support staff for their efforts.

## References

- [1] Conceptual design report, section 2, Gesellschaft für Schwerionen Forschung, 2001; also [http://www.gsi.de/zukunftsprojekt/index\\_e.html](http://www.gsi.de/zukunftsprojekt/index_e.html)
- [2] G. Savard, in AIP-Conference-Proceedings **656**, (2003) 335; also <http://www.nsl.msu.edu/ria/>
- [3] Report of the SPIRAL 2 Detailed Design Study (APD), GANIL 2005; also <http://www.ganil.fr/research/developments/spiral2/whatisspiral2.html>
- [4] B. Harras et al., Rev. Sci. Instr. **71** (2000) 380.

- [5] R.E. Tribble, C.A. Gagliardi, and W. Liu, Nucl. Instr. Meth. B **56/57** (1991) 956.
- [6] H.W. Wilschut, Hyperfine Interactions 146(2003)77;  
H.W. Wilschut in AIP conference proceedings 802 (2005) 223;  
K. Jungmann et al., Physica Scripta T104(2003)178;  
M. Sohani, Acta Physica Polonica B37(2006)231.
- [7] G.P.A. Berg et al., Nucl. Instr. and Meth. **A560** (2006) 169.
- [8] L. Achouri et al. in KVI annual report 2005 p. 13
- [9] S.G. Pedersen et al., to appear in Proceedings of Science (PoS) and M.J.G. Borge et al. in KVI annual report 2005 p. 12.
- [10] D.Bazin et al. Nucl. Instr. and Meth. A482 (2002) 307. Nucl. Instr. and Meth. A 257 (1987) 215.
- [11] B.M. Sherrill, et al. Nucl. Instr. and Meth. B 56/57 (1991) 1106.
- [12] J.F. Brinkley et al. in Cyclotron Institute of Texas A&M Universtiy Progress in Research, 2004 section V-9.
- [13] A.R. Young et al. in KVI annual report 2004 p.17.
- [14] R.F. Bentley, thesis, Colorado University, 1972.
- [15] A. Terakawa et al., Phys. Rev. C 48 (1993) 2775.
- [16] T.N. Taddeucci et al., Nucl. Phys. A469 (1987) 125.
- [17] T.N. Taddeucci et al., Phys. Rev. C 41(1990)2548.
- [18] O. Tarasov and D. Bazin, Nucl. Phys. A 746(2004)411.